The evolving genetic and pathophysiological spectrum of migraine

Vries, B. de

7.0

RNA expression profiles of familial hemiplegic migraine type 1 mouse models with relevance to migraine-associated cerebellar ataxia

B. de Vries, MSc[1], L.A.M. Broos, BSc[1], P.A.C. 't Hoen, PhD[1], S.C. Koelewijn, BSc[1], B. Todorov, MSc[1], M.D. Ferrari, MD, PhD[2], J.M. Boer, PhD[1], R.R. Frants, PhD[1], A.M.J.M. van den Maagdenberg, PhD[1,2]

[1]Department of Human Genetics, Leiden University Medical Centre, Leiden, The Netherlands
[2]Department of Neurology, Leiden University Medical Centre, Leiden, The Netherlands

Manuscript in preparation

Abstract

The *CACNA1A* gene encodes the α1 subunit of voltage-gated $Ca_V2.1$ calcium channels. Several mutations in *CACNA1A* are associated with familial hemiplegic migraine (FHM), a rare monogenic subtype of migraine with aura that can be accompanied by cerebellar ataxia and/or epilepsy. Two extremes of the FHM clinical spectrum are seen with missense mutations R192Q and S218L. Whereas patients with the R192Q mutation suffer from pure FHM without additional neurological features, S218L patients show a particularly severe phenotype with FHM, cerebellar ataxia, seizures, and brain edema after a mild head trauma. Recently, transgenic knock-in (KI) *Cacna1a* mouse models were generated that carry either the R192Q or the S218L mutation. Here we investigated their RNA expression profiles under basal conditions in the occipital cortex and the cerebellum because of their relevance to the aura and ataxia, respectively. Expression differences were most pronounced in the cerebellum of S218L mice and could be linked to their ataxic phenotype, qPCR was used to validate these results. Remarkably, tyrosine hydroxylase, a marker of delayed cerebellar maturation, is strongly up-regulated in the cerebellum of S218L mice, which was confirmed by immunohistochemistry. In addition, neuronal pathways, such as neurotransmitter synthesis pathways are up-regulated in the cerebellum of S218L mice. In contrast, only modest differences in expression profiles were observed in the cortex of both KI mice, despite pronounced consequences at the molecular and neurobiological level. Our findings indicate that the migraine-associated phenotype cerebellar ataxia is reflected in the basal RNA expression profiles.

Introduction

Familial hemiplegic migraine (FHM) is a rare Mendelian subtype of migraine with aura that is characterized by transient hemiparesis during the aura phase.[1] FHM is considered a relevant model for the common forms of migraine, because, (i) apart from the hemiparesis, the aura and headache features are identical to those in non-hemiplegic migraine types[2], and (ii) many patients also have non-hemiplegic migraine attacks.[3-5] Three FHM genes have been identified that all encode subunits of ion transporters.[6] The FHM1 gene, *CACNA1A*, encodes the pore-forming α1 subunit of voltage-gated $Ca_V2.1$ calcium channels that are located mainly at presynaptic terminals throughout the central nervous system where they regulate neurotransmitter release.[7] $Ca_V2.1$ channels are expressed throughout the brain, but are particularly high expressed in the cerebellum.[8] FHM1 mutations can be associated with pure FHM, such as in R192Q mutation carriers[9], or can be complex and severe with FHM and associated cerebellar ataxia, seizures, mild head trauma-induced cerebral edema, and even fatal coma, in patients with the S218L mutation.[10,11]

The migraine aura is caused by cortical spreading depression (CSD), a wave of neuronal and glial cell depolarization that originates in the occipital cortex and slowly propagates over the brain cortex.[17,13] The headache phase likely results from an activation of the trigeminovascular system (TGVS)[14], a system that consists of the neurons innervating the cerebral vessels. In animal studies, CSD was shown to activate the TGVS and thereby headache mechanisms.[15] Of the associated neurological phenotypes, the cause of cerebellar ataxia is most clear. Evidence from natural *Cacna1a* mouse mutants revealed that an irregularity in the firing of cerebellar Purkinje cell neurons is the likely underlying cause.[16,17] Notably, subclinical cerebellar signs were observed in migraine patients and found more pronounced in migraine with aura than in migraine without aura.[18]

To investigate the neurobiological consequences of FHM1 mutations, transgenic *Cacna1a* knock-in (KI) mouse models were generated that either carry the FHM1 R192Q or the S218L mutation.[19,20] Whereas S218L KI mice show a similar, complex, phenotype as S218L patients, the R192Q KI mice do not exhibit an overt behavioral phenotype. At the neurobiological level, however, both KI mouse mutants show multiple *gain-of-function* effects, such as an increased neuronal calcium influx, increased neurotransmitter release, and enhanced susceptibility to cortical spreading depression (CSD); all of which are more pronounced in S218L mice.[19-21] Here we investigated the RNA expression profiles in the occipital cortex (the origin of CSD and the aura) and the cerebellum (the origin of the ataxia) to investigate whether molecular changes are associated with the pathophysiology of at least some of the migraine-associated clinical features. Expression profiles were shown to be remarkably stable, and specific differences in gene expression were demonstrated that could be linked to ataxia-relevant pathways.

Materials and Methods

Animals

Transgenic knock-in (KI) mice were generated by gene targeting of the *Cacna1a* gene that carry either the human FHM1 R192Q or S218L mutation, in which the neomycin selection cassette was removed by in vivo deletion by crossing the KI mice with Cre deleter mice.[19,20] Homozygous KI mice and wild-type mice of both genders aged 7-10 weeks were used. KI mice were backcrossed with C57BL/6J for five (R192Q) and for three (S218L) generations. Each group consisted of six mice (biological replicates), unless mentioned otherwise (Table 1). Confirmatory genotyping was performed by PCR analysis on genomic DNA from tail biopsies. Animal care and procedures were approved by the local ethical committee according to national guidelines.

Table 1 *Experimental groups of mice*

Genotype	Brain structure	Gender (n)
Wild-type mice	Cerebellum	Male (6)
		Female (6)
	Occipital cortex	Male (6)
		Female (6)
S218L knock-in mice	Cerebellum	Male (6)
		Female (5)
	Occipital cortex	Male (6)
		Female (5)
R192Q knock-in mice	Cerebellum	Male (6)
	Occipital cortex	Male (n=6)

Dissections of brain structures

Animals were sacrificed by cervical dislocation and brains were rapidly removed from the skull. Brain material was dissected and snap-frozen in liquid nitrogen within 15 minutes and stored at -80°C until RNA isolation. Brain material was dissected in nine parts: the cerebellum (in two halves), both hemispheres of the cortex (with each hemisphere further dissected in three parts, one containing the occipital cortex), and the brainstem.

RNA isolation

The right half of the cerebellum and the occipital third of the right cortex were chosen for expression profiling. For total RNA isolation, the Macherey Nagel RNA isolation kit (Düren, Germany) was used in combination with an Ultra-turrax T25 Polytron (Janke & Kunkel, Staufen, Germany) mechanical homogenizer. In brief, frozen tissue was crunched using a mortar under liquid nitrogen. Subsequently, tissue was homogenized in lysis buffer using the Polytron. Total RNA was bound to silica membrane of Macherey Nagel columns, while contaminating DNA was removed by rDNase. At the end of the procedure, total RNA was eluted with RNase-free water. RNA integrity was determined using the Agilent 2100 Bioanalyzer total RNA nanochips (Agilent, Foster City, USA, CA). All RNA samples that were included in the study had a minimal RIN (RNA integrity number) value of 7.0.

Gene expression profiling using Illumina microarrays

Biotin-labelled cRNA was produced using a linear amplification kit (IL1791; Ambion, Austin, USA, TX) using 300 ng of total RNA as input. cRNA samples were hybridized on Illumina mouse-6 Bead Chips, which contain 44,505 probe IDs. Chip hybridizations, washing, Cy3-streptavidin (Amersham Biosciences, Uppsala, Sweden) staining, and scanning were performed on an Illumina Bead Station 500 platform (San Diego, http://www.illumina.com) using reagents and protocols supplied by the manufacturer.

Gene expression profile data analysis

Resulting data files were loaded into Rosetta Resolver version 7.2 (Rosetta Biosoftware, Seattle, WA). Raw data were normalized using the standard Rosetta error model for Illumina arrays. Differences in gene expression between groups were evaluated using an error-weighted two-way analysis of variance with genotype and gender as factors and Benjamini-Hochberg FDR was used for multiple testing corrections (FDR, $P < 0.05$). Post-hoc analysis was performed using Tukey-Kramer (FDR, $P < 0.05$). Cerebellum and occipital cortex profiles were analyzed separately. A 'cortical' signature representing genes that are differently expressed in the cortex of both mutant mice was selected based on ANOVA statistics and post-hoc analysis. Genes with a significant ANOVA *P*-value for the parameter genotype, and that based on the post-hoc analysis were differently expressed between mutant mice (both S218L and R192Q) and wild-type mice were selected. Similarly, an 'ataxia' signature was created that represents genes that were differently expressed in the cerebellum of the S218L mice. Using the Ontologizer program (http://compbio.charite.de/index.php/ontologizer2.html) function labels were ascribed to each gene. Genes were grouped into categories according to these function labels to determine over- or underrepresentation of certain categories. These over-or underrepresentation analyses were only performed on gene sets containing over 100 genes.

Literature-based relationships

Literature-based relationships between genes in the specific gene sets and migraine were studied using the Anni text-mining program (Anni version 2.1).[22] For each gene or disorder a concept profile was generated by the program. A concept profile is a summary of all concepts directly co-mentioned with the disease or gene concept (i.e. the main concept) in PubMed abstracts. The strength of association for each concept with the main concept is calculated using 2x2 contingency tables and the uncertainty coefficient. The association between two concept profiles is calculated using vector based matching (e.g. inner product score) over the concepts that the two profiles have in common.

Quantitative RT-PCR

The same RNA samples were used for evaluation of microarray results by quantitative PCR (qPCR). Genes that were selected for qPCR had a fold-change of at least 1.3 and detectable expression levels. First-strand cDNA was synthesized using random hexamer primers. Subsequently, qPCRs were performed on the MyiQ™ Single-Color Real-Time PCR Detection System (Bio-Rad, Hercules, USA, CA) using gene-specific primers (Supplemental Table 1). cDNAs were analyzed in duplicate, after which the average cycle threshold (Ct) was calculated per sample. To correct for input differences between mutant and wild-type samples, Ct values were corrected per tissue for the differences in housekeeping gene *Gapdh* expression. Differential expression was calculated using Student's *t*-test.

Immunohistochemistry of tyrosine hydroxylase

Mice were anaesthetized with Nembutal (50 mg/kg, i.p.) and perfused intracardially with phosphate buffered saline (PBS) followed by 4% paraformaldehyde in 0.1 M phosphate buffer (pH 7.4). Post-fixation was performed for 2 h in 4% buffered paraformaldehyde followed by overnight incubation in 10% sucrose in 0.1 M phosphate buffer at 4°C. Next, tissue was embedded in 10% sucrose with 11% gelatin, fixed with 30% sucrose in 4% buffered paraformaldehyde for 2.5 h at room temperature, followed by overnight incubation in 30% sucrose in 0.1 M phosphate at 4 °C. Tissue was cut into 40 µm sagittal sections and processed for free-floating immunohistochemistry. Briefly, sections were incubated in 10% heat-inactivated normal horse serum, 0.5% Triton X100 in Tris-buffered saline (TBS) for 2 h and then incubated with primary rabbit anti-tyrosine hydroxylase antibody (AB152, 1:2,000; Chemicon, Temecula, USA, CA), diluted in TBS containing 1% normal horse serum, 0.4% Triton X100 at 4 °C. Secondary biotin-labeled goat anti-rabbit antibody (1:200; Vector Laboratories, Burlingame, USA, CA) incubation was performed for 2 h at room temperature. Finally, for detection, sections were incubated with the avidin-biotin kit (Vector Laboratories) for 2 h at room temperature, washed, and developed in 0.1 mg/ml diaminobenzidine with 0.005% H_2O_2.

Single Nucleotide Polymorphism analysis

Using the Mouse Genome Informatics (MGI) database (http://www.informatics.jax.org/), SNPs surrounding the *Cacna1a* locus on mouse chromosome 8 were selected that could distinguish C57BL/6J- and 129/Ola-derived sequences. Using genomic tail DNA, SNP genotypes for all mutant mice that were included in the study were determined by standard PCR combined with direct sequencing.

Results

Here we studied RNA expression profiles of cerebellar and occipital cortex tissue of two *Cacna1a* KI mouse models of migraine. In line with data from previous studies that revealed similar $Ca_V2.1$ α1 protein expression levels between genotypes[19,20], *Cacna1a* RNA expression levels were similar between genotypes, except for an apparent down-regulation of *Cacna1a* (Fold change -1.25; $P = 0.01$) in cerebellum of R192Q mice (Table 2). No other meaningful genotypic differences were detected in gene expression levels of Ca_V auxiliary subunits (i.e., β1-4, γ1-8 and α2δ1-3), except for minor differences in *Cacnb1*, *Cacnb3* and *Cacnb4* and in *Cacng7* in the occipital cortex of S218L mice (Supplementary Table 2).

Table 2 *Expression levels of genes encoding pore-forming subunits of Ca_v channels*

Gene	Cerebellum R192Q	Cerebellum S218L	Occipital cortex R192Q	Occipital cortex S218L
Cacna1a	-1.29 (0.02)*	-1.13 (0.19)	-1.24 (0.06)	-1.11 (0.37)
Cacna1b	-1.06 (0.27)	1.01 (0.90)	-1.08 (0.28)	1.00 (0.97)
Cacna1c	-1.13 (0.08)	-1.04 (0.60)	-1.04 (0.62)	-1.08 (0.38)
Cacna1d	-1.05 (0.67)	1.21 (0.09)	-1.04 (0.86)	-1.01 (0.94)
Cacna1e	1.01 (0.96)	-1.11 (0.50)	-1.12 (0.52)	-1.03 (0.85)
Cacna1f	1.06 (0.62)	-1.03 (0.76)	-1.08 (0.56)	1.06 (0.71)
Cacna1g	-1.05 (0.57)	-1.08 (0.27)	-1.03 (0.93)	1.12 (0.69)
Cacna1h	1.02 (0.84)	1.42 (0.004)*	1.03 (0.74)	1.07 (0.48)
Cacna1i	1.02 (0.80)	-1.01 (0.81)	-1.07 (0.36)	-1.01 (0.82)
Cacna1s	1.18 (0.09)	1.06 (0.52)	-1.09 (0.36)	1.03 (0.82)

*Numbers represent the mean fold-change for each gene transcript seen in the respective mutant mice compared to wild-type mice; P-value for this fold change is indicated between the brackets. *Fold-change with a $P < 0.05$.*

To further assess gene expression profiles in *Cacna1a* KI and wild-type mice, a two-way ANOVA was performed for cerebellum and cortex separately, with genotype and gender as factors. The effect of gender was not remarkable. In the cerebellum, only 16 genes were significantly differentially expressed between males and females; for the occipital cortex only 10 genes were significantly differentially expressed. For both the cerebellum and occipital cortex, a large portion of significantly differentially expressed genes (DEGs) between genotypes are located on chromosome 8, which contains the *Cacna1a* gene that was modified by gene targeting. Although KI mice and wild-type mice were backcrossed with C57BL/6J for several generations, the region directly flanking the *Cacna1a* gene remained of 129 genetic background. It is therefore unclear whether the 'chromosome 8 genes' are differently expressed because of the presence of an FHM1 mutation or a different genetic background.[23] To investigate this further, we determined the genomic boundaries of 129-derived chromosome 8 regions in the FHM1 mice. The 129-derived region flanking the *Cacna1a* gene extended maximally 37 Mb upstream to 46 Mb downstream of the R192Q mutation and 37 Mb upstream and 52 Mb downstream of the S218L mutation. As the 129-derived region covered most of chromosome 8 in at least some of the mice, we decided to exclude all genes located on chromosome 8 from the gene signatures used for subsequent analyses.

After chromosome 8 exclusion, only 22 DEGs remained for the occipital cortex of R192Q KI mice. For S218L KI mice, only 10 genes were differentially expressed in the occipital cortex. Notably, without chromosome 8 exclusion 61 and 67 DEGs were observed for R192Q KI and S218L KI mice, respectively. However, in the cerebellum, the number of DEGs after chromosome 8 exclusion was

considerably higher: 82 for R192Q KI and 335 for S218L KI mice. We believe that the relatively low number of DEGs is not due to lack of power, given the fact that our experiment easily picked up genes from the chromosome 8 region with relatively subtle changes in gene expression.

Because the occipital cortex is most relevant for the observed increased susceptibility to cortical spreading depression (CSD) in KI mice, we selected a 'cortical' gene signature by selecting genes that were differentially expressed in the occipital cortex of both mutant mice models (figure 1A). Notably, nine out of 10 DEGs were differentially expressed in both strains of mutant mice (Table 3); all showing only modest fold-changes. Six genes (i.e., *Lsm10*, *Gpr34*, *Gpr23*, *Ctxn3*, *Gli3* and *Tnnc1*) were up-regulated in both strains, whereas one gene (*Cort*) was up-regulated in one and down-regulated in the other; two genes (i.e., *Camkk1* and *Tom1l2*) were down-regulated in both strains.

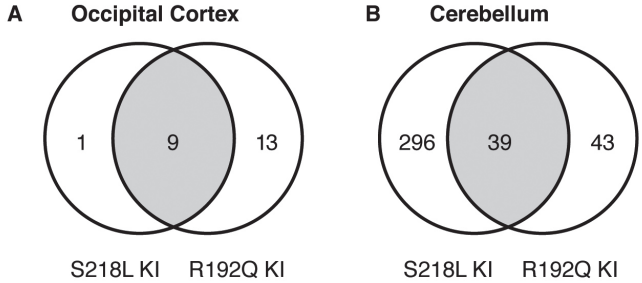

Figure 1 A. *Differentially expressed genes in the occipital cortex of mutant KI mice. Only nine genes are differentially expressed in the occipital cortex of both KI mouse models ('cortical' signature). B Differentially expressed genes in cerebellum. No less than 296 genes are differentially expressed in the cerebellum of S218L KI mice compared to R192Q KI and wild-type mice ('ataxia' signature).*

Table 3 *Genes that are differentially expressed in the occipital cortex of both R192Q and S218L mice ('cortical' signature)*

Genes	Description	P-value ANOVA (parameter genotype)	Fold change (S218L vs wild-type)	Fold change (R192Q vs wild-type)
Camkk1	calcium/calmodulin-dependent protein kinase kinase 1, alpha	3.80×10^{-6}	-1.06 (0.05)	-1.29 ($4.04.10^{-16}$)
Cort	Cortistatin	0.01	-1.17 (0.02)	1.19 (3.1×10^{-3})
Ctxn3	cortexin 3	8.33×10^{-3}	1.25 (2.1×10^{-4})	1.35 (2.20×10^{-8})
Gli3	GLI-Kruppel family member GLI3	0.03	1.16 (2.4×10^{-3})	1.28 (2.1×10^{-4})
Gpr23	G protein-coupled receptor 23	0.04	1.26 (1.1×10^{-3})	1.38 (5.51×10^{-6})
Gpr34	G protein-coupled receptor 34	6.08×10^{-8}	1.34 (5.5×10^{-10})	1.43 (9.44×10^{-12})
Lsm10	U7 snRNP-specific Sm-like protein	0.03	1.12 (9.0×10^{-4})	1.16 (4.80×10^{-4})
Tnnc1	troponin C, cardiac/slow skeletal	0.03	1.19 (0.04)	1.45 (4.0×10^{-5})
Tom1l2	target of myb1-like 2 (chicken)	2.53×10^{-3}	-1.47 (2.0×10^{-5})	-1.53 (1.33×10^{-7})

Numbers represent the mean fold-change for each gene transcript seen in the respective mutant mice compared wild-type mice. The numbers in brackets represent the P-value for the respective fold change.

Also for the cerebellum, from which the cerebellar ataxia originates, we extracted a signature (i.e., 'ataxia' gene signature) containing genes that were differentially expressed in the cerebellum of S218L KI mice (compared to R192Q KI and wild-type mice). The 'ataxia' signature contained 296 genes (Figure 1B). Using the Ontologizer program, a GO term analysis was performed for under- or over-representation of functional categories and yielded significant overrepresentation of four biological processes GO terms (Table 4). All four were related to neurotransmitter synthesis. Subsequently, qPCR analyses were performed for five DEGs from these pathways and essentially confirmed the findings of the microarray experiments (Figure 2). Using the Anni text-mining program we investigated possible literature-based relationships between the term ataxia and the genes in the 'ataxia' gene signature. The *Ppp2r2b* gene, encoding brain-specific regulatory subunit of the protein phosphatase PP2A, and the *Gfap* gene, encoding glial fibrillary acidic protein, showed most obvious literature-based relationships with ataxia. *Ppp2r2b* and *Gfap* were both upregulated in the cerebellum of the S218L KI mice with a fold-change of 1.2 ($P = 6.4x10^{-4}$) and 1.6 ($P = 2.9x10^{-4}$), respectively.

Table 4 *Pathways that were significantly overrepresented in the 'ataxia' gene signature (P < 0.05 after Benjamini-Hochberg correction for multiple testing)*

Gene Symbol	Gene Description	Fold change (*P*-value)
GO:0042401 biogenic amine biosynthetic process		
Agmat	Agmatine ureohydrolase (agmatinase)	2.71 (4.27×10^{-9})
Ddc	Dopa decarboxylase	1.26 (7.60×10^{-4})
Hdc	Histidine decarboxylase	-1.92 (4.73×10^{-7})
Th	Tyrosine hydroxylase	13.12 (3.92×10^{-20})
Tph2	Tryptophan hydroxylase 2	1.58 (6.90×10^{-4})
GO:0042398 amino acid derivative biosynthetic process		
Agmat	Agmatine ureohydrolase (agmatinase)	2.71 (4.27×10^{-9})
Ddc	Dopa decarboxylase	1.26 (7.60×10^{-4})
Hdc	Histidine decarboxylase	-1.92 (4.73×10^{-7})
Th	Tyrosine hydroxylase	13.12 (3.92×10^{-20})
Tph2	Tryptophan hydroxylase 2	1.58 (6.90×10^{-4})
GO:0042423 catecholamine biosynthetic process		
Ddc	Dopa decarboxylase	1.26 (7.60×10^{-4})
Hdc	Histidine decarboxylase	-1.92 (4.73×10^{-7})
Th	Tyrosine hydroxylase	13.12 (3.92×10^{-20})
GO:0042136 neurotransmitter biosynthetic process		
Gad2	Glutamic acid decarboxylase 2	1.20 (2.00×10^{-5})
Th	Tyrosine hydroxylase	13.12 (3.92×10^{-20})
Tph2	Tryptophan hydroxylase 2	1.58 (6.90×10^{-4})

Output generated using Ontologizer programm

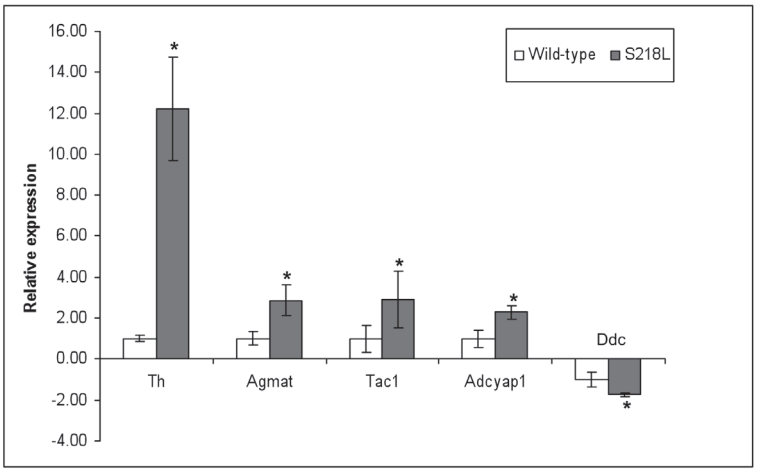

Figure 2. *Quantitative PCR analysis of genes altered in the cerebellum of S218L mice. Data are expressed as fold changes (means ± SD), normalized to Gapdh mRNA expression, where the values for wild-type mice were set at 1.00 or -1.00. * P < 0.05 compared to the wild-type mice.*

The most striking fold-change in the 'ataxia' gene signature was seen for tyrosine hydroxylase (*Th*) (fold-change 13.1; $P = 3.92 \times 10^{-20}$). Th up-regulation was also observed at the protein level, as evidenced by strong immunoreactivity in a considerable number of Purkinje cells specifically in the cerebellum of S218L mice (Figure 3).

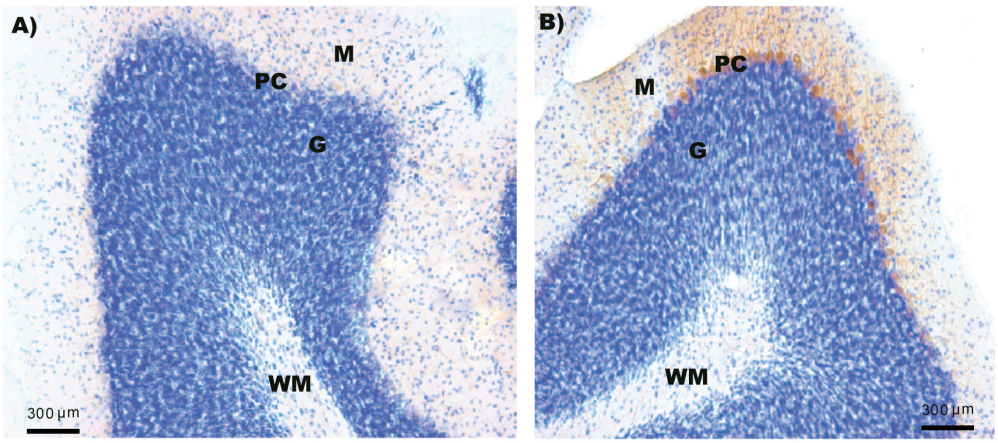

Figure 3. *Protein expression of tyrosine hydroxylase (Th) in the cerebellum. Immunohistochemistry using Th-specific antibody (brown signal). Some Purkinje cells stain positive in the S218L mutant. Left panel: wild-type, right panel: S218L. M: molecular layer, PC: Purkinje cell layer, G: Granule cell layer, WM: white matter.*

Discussion

Here we performed the first gene expression study in transgenic KI mouse models carrying human pathogenic FHM1 mutations R192Q and S218L in an attempt to increase our insight in the molecular consequences of these mutations in migraine pathophysiology.

Despite considerable insight in the pathophysiology of migraine attacks, it is still largely unknown how attacks begin and to what extent the migraine brain is different from a healthy brain. Therefore, we studied RNA expression profiles of brains of migraine mouse models under basal conditions. We investigated the third most caudal part of the cortex (that includes the visual cortex) because CSD, the electrophysiological substrate of the migraine aura, originates in this area of the cortex.[13] In addition, we studied the cerebellum because cerebellar ataxia originates from this area of the brain and cerebellar ataxia is a prominent part of the phenotype of S218L mice.

In line with earlier studies on these mouse models that revealed unchanged numbers of functional $Ca_V2.1$ channels at the plasma membrane[19,20], mRNA expression levels of the mutated *Cacna1a* gene were relatively similar between genotypes. Therefore, FHM1 mutations do not seem to affect this gene at the RNA level. Similarly, no clear changes in gene expression levels were observed for other subunits of Ca_V channels. Consequently, we postulate that the clinical features seen in mice and patients with FHM1 gene mutations are likely more the result of changed functionality of $Ca_V2.1$ channels, perhaps in combination with changes in downstream targets of these channels.

As both KI mutants were generated on a mixed C57BL/6J x 129SvEv genetic background[19,20], despite being back-crossed to C57BL/6J for several generations, one should take into account that gene sequences on chromosome 8 that flank the mutated *Cacna1a* gene are still of 129 origin. Valor and Grant have shown that remnant 129 sequences may lead to gene expression differences because of mixed genetic differences at this location.[23] Indeed, when comparing expression profiles from mutant KI and wild-type mice, we observed a much higher than expected frequency of DEGs located in close proximity of the mutated *Cacna1a* gene. Unlike what was reported in their study, no selection cassette, which is known to profoundly affect expression of neighbouring genes, was present in our mice. Therefore, in our study it is more likely that gene expression differences are the direct consequence of subtle differences in genetic background (i.e., 129Sv vs. Bl6). Although we do not have any evidence for it, we postulate that perhaps the presence of 32-bp LoxP sequences that are still present in the targeted locus, might have a cis-effect on gene expression of neighbouring genes.

Although molecular and electrophysiological studies have shown that neuronal excitability is increased in the KI mutants, we could show that this is not accompanied with prominent gene expression changes in the occipital cortex (at least under unchallenged conditions). In fact, only *nine* genes were differentially expressed in the cortex of mutant KI mice. In contrast, many expression differences were observed in the cerebellum of the mutant KI mice; especially in the cerebellum of the S218L mice. This may be expected since mice (and patients) with the S218L mutation suffer from cerebellar ataxia. GO term analysis with the S218L-specific 'ataxia' gene signature showed significant overrepresentation of genes belonging to pathways involved in neurotransmitter synthesis. Especially catecholamine neurotransmitter (i.e., dopamine and serotonin) pathways were differentially expressed.

In the S218L-specific 'ataxia' gene signature, the largest fold-change was observed for the tyrosine hydroxylase (*Th*) gene, which encodes the rate-limiting enzyme of the biosynthetic pathway of catecholamines, dopamine, norepinephrine and epinephrine.[24] Th overexpression was confirmed at the protein level with immunohistochemistry (Figure 3). Th is transiently expressed in the cerebellum during development, but absent (or very low expressed) in the cerebellum of adult mice.[25] Hence, Th expression in the adult cerebellum is considered a marker for delayed maturation of the cerebellum. Interestingly, also other ataxic mouse models with natural *Cacna1a* mutations (i.e., *Rolling Nagoya*, *Tottering*, and *Leaner*) show a high, persistent Th expression in the adult cerebellum.[26-28] However, as phosphorylation of several serine residues is absent in up-regulated Th in these mice, but important for Th activity[29,30], it is unclear whether also Th function is abnormal in *Cacna1a* mutant mice. Notably, a recent expression profiling study in *Purkinje cell degeneration* mice, which are characterized by degeneration of cerebellar Purkinje cells and progressive ataxia, showed a 2-fold increase in expression of the *Th* gene.[31]

Several genes in the S218L-specific 'ataxia' gene signature can be linked to cerebellar ataxia relevant pathways. For example 5' non-coding CAG expansions in the *PPP2R2B* gene, which encodes a brain-specific regulatory subunit of the protein phosphatase PP2A holoenzyme, cause spinocerebellar ataxia type 12 (SCA12).[32] The repeat expansion leads to increased PPP2R2B expression[33], similar to what was found in the cerebellum of the S218L KI mice. In addition, mutations in glial fibrillary acidic protein (GFAP) are associated with infantile and juvenile Alexander disease; a rare leukodystrophy of the cerebellum.[34] Gait ataxia is a common clinical feature in patients with adult-onset Alexander disease.[35-37]

In conclusion, the occipital cortex of the KI mouse models of migraine did not show prominent expression differences. The transcriptome of the occipital cortex in migraine mice was remarkably stable. This enables future profiling studies that aim to investigate the consequences on RNA expression of triggers relevant to migraine. On the other hand, certain differences in RNA expression profiles of the cerebellum of the S218L KI mice could be linked to ataxia.

Acknowledgements

This work was supported by grants of the Netherlands Organization for Scientific Research (NWO) (Vici 918.56.602, M.D.F), the EU "EUROHEAD" grant (LSHM-CT-2004-504837; M.D.F, R.R.F, A.M.J.M.v.d.M) and the Centre of Medical Systems Biology (CMSB) established by the Netherlands Genomics Initiative/Netherlands Organisation for Scientific Research (NGI/NWO).

References

1. Headache classification subcommittee of the international headache society. The international Classification of Headache Disorders. 2nd Edition. *Cephalalgia* 2004;24:1-160.

2. Thomsen LL, Eriksen MK, Roemer SF et al (2002) A population-based study of familial hemiplegic migraine suggests revised diagnostic criteria. *Brain* 125:1379-1391.

3. Terwindt GM, Ophoff RA, Haan J et al (1998) Variable clinical expression of mutations in the P/Q-type calcium channel gene in familial hemiplegic migraine. Dutch Migraine Genetics Research Group. *Neurology* 50:1105-1110.

4. Ducros A, Dernier C, Joutel A et al (2001) The clinical spectrum of familial hemiplegic migraine associated with mutations in a neuronal calcium channel. *N Engl J Med* 354:17-24.

5. Thomsen LL, Ostergaard E, Romer SF et al (2003) Sporadic hemiplegic migraine is an aetiologically heterogeneous disorder. *Cephalalgia* 23:921-928.

6. van den Maagdenberg AM, Haan J, Terwindt GM, Ferrari MD (2007) Migraine: gene mutations and functional consequences. *Curr Opin Neurol* 20:299-305.

7. Mintz IM, Sabatini BL, Regehr WG. Calcium control of transmitter release at a cerebellar synapse. *Neuron* 1995 15:675-688.

8. Craig PJ, McAinsh AD, McCormack AL et al (1998) Distribution of the voltage-dependent calcium channel alpha (1A) subunit throughout the mature rat brain and its relationship to neurotransmitter pathways. *J Comp Neurol* 27;397:251-267.

9. Ophoff RA, Terwindt GM, Vergouwe MN et al. Familial hemiplegic migraine

and episodic ataxia type-2 are caused by mutations in the $Ca2^{+}$ channel gene CACNL1A4. *Cell* 1996;87:543-552.

10. Kors EE, Terwindt GM, Vermeulen FL et al (2001) Delayed cerebral edema and fatal coma after minor head trauma: role of the CACNA1A calcium channel subunit gene and relationship with familial hemiplegic migraine. *Ann Neurol* 49:753-760.

11. Stam AH, Luijckx GJ, Poll-The BT et al (2009) Early seizures and cerebral edema after trivial head trauma associated with the CACNA1A S218L mutation. *J Neurol Neurosurg Psychiatry*. 80(10):1125-1129.

12. Leao, A.A.P. 1944. Spreading depression of activity in cerebral cortex. *J Neurophysiol* 7:359–390.

13. Somjen, GG 2001. Mechanisms of spreading depression and hypoxic spreading depression-like depolarization. *Physiol Rev* 81:1065–1096.

14. Messlinger K (2009) Migraine: where and how does the pain originate? *Exp Brain Res* 196:179-193.

15. Bolay H, Reuter U, Dunn AK et al (2002) Intrinsic brain activity triggers trigeminal meningeal afferents in a migraine model. *Nat Med* 8:136-142.

16. Hoebeek FE, Stahl JS, van Alphen AM, Schonewille et al (2005) Increased noise level of purkinje cell activities minimizes impact of their modulation during sensorimotor control. *Neuron* 24;45:953-965.

17. Walter JT, Alviña K, Womack MD et al (2006) Decreases in the precision of Purkinje cell pacemaking cause cerebellar dysfunction and ataxia. *Nat Neurosci* 9:389-397.

18. Sándor PS, Mascia A, Seidel et al (2001) Subclinical cerebellar impairment in the common types of migraine: a three-dimensional analysis of reaching movements. *Ann Neurol* 49(5):668-672.

19. van den Maagdenberg AM, Pietrobon D, Pizzorusso T et al (2004) A Cacna1a knockin migraine mouse model with increased susceptibility to cortical spreading depression. *Neuron* 41:701-710.

20. van den Maagdenberg AM, Pizzorusso T, Kaja S et al (2010) High CSD susceptibility and migraine-associated symptoms in CaV2.1 S218L mice *Ann Neurol* 67:85-98.

21. Tottene A, Conti R, Fabbro A et al (2009) Enhanced excitatory transmission at cortical synapses as the basis for facilitated spreading depression in Ca(v)2.1 knockin migraine mice. *Neuron* 12:762-773.

22. van Haagen HH, 't Hoen PA, Botelho Bovo A, de Morrée A et al (2009) Novel protein-protein interactions inferred from literature context. *PLoS One* 18;4(11):e7894.

23. Valor LM, Grant SG. (2007) Clustered gene expression changes flank targeted gene loci in knockout mice. *PLoS ONE* 12;2(12):e1303.

24. Moy LY, Tsai LH (2004). Cyclin-dependent kinase 5 phosphorylates serine 31 of tyrosine hydroxylase and regulates its stability. *J Biol Chem* 279:54487-54493.

25. Jeong YG, Kim MK, Hawkes R (2001). Ectopic expression of tyrosine hydroxylase in Zebrin II immunoreactive Purkinje cells in the cerebellum of the ataxic mutant mouse, pogo. *Brain Res Dev Brain Res* 23:201-209.

26. Austin MC, Schultzberg M, Abbott LC et al (1992) Expression of tyrosine hydroxylase in cerebellar Purkinje neurons of the mutant tottering and leaner mouse. *Brain Res Mol Brain Res* 15:227-240.

27. Abbott LC, Isaacs KR, Heckroth JA (1996) Co-localization of tyrosine hydroxylase and zebrin II immunoreactivities in Purkinje cells of the mutant mice, tottering and tottering/leaner. *Neuroscience* 71:461-475.

28. Sawada K, Komatsu S, Haga H et al (1999) Abnormal expression of tyrosine hydroxylase immunoreactivity in Purkinje cells precedes the onset of ataxia in dilute-lethal mice. *Brain Res* 9;844:188-191.

29. Daubner SC, Lauriano C, Haycock JW, Fitzpatrick PF (1992) Site-directed mutagenesis of serine-40 of rat tyrosine hydroxylase, effects of dopamine and cAMP-dependent phosphorylation on enzyme activity. *J Biol Chem* 267:12639-12646.

30. Kaufman S (1995) Tyrosine hydroxylase. *Adv Enzymol Relat Areas Mol Biol* 70:103-220.

31. Ford GD, Ford BD, Steele EC (2008) Analysis of transcriptional profiles and functional clustering of global cerebellar gene expression in PCD3J mice. *Biochem Biophys Res Comm* 377:556–561.

32. Holmes S. E., O'Hearn E. E., McInnis M. G. et al (1999) Expansion of a novel CAG trinucleotide repeat in the 5' region of PPP2R2B is associated with SCA12. *Nat Genet* 23:391–392.

33. Sowell ER, Levitt J, Thompson PM et al (2000) Brain abnormalities in early-onset schizophrenia spectrum disorder observed with statistical parametric mapping of structural magnetic resonance images. *Am J Psychiatry* 157:1475–1484.

34. Borrett D, Becker LE (1985) Alexander's disease: A disease of astrocytes. *Brain* 108:367–385.

35. Namekawa M, Takiyama Y, Aoki Y et al (2002) Identification of GFAP gene mutation in hereditary adult-onset Alexander's disease. *Ann Neurol* 52:779-785.

36. Brockmann K, Meins M, Taubert A et al (2003) A Novel GFAP Mutation and Disseminated White Matter Lesions: Adult Alexander Disease? *Eur Neurol* 50:100-105.

37. Kaneko H, Hirose M, Katada S et al (2009) Novel GFAP mutation in patient with adult-onset Alexander disease presenting with spastic ataxia. *Mov Disord* 15:1393-1395.

Supplementary Tables

Supplemental Table 1. *Primers used for qPCR*

Gene symbol	Gene description	Primer sequence	Amplicon size
Adcyap1	Adenylate cyclase activating polypeptide 1	F 5′-TTTCCTAGACACCAATGACCA-3′	79 bp
		R 5′-GACACTGCTATGCATTATTATCCC-3′	
Agmat	Agmatine ureohydrolase (agmatinase)	F 5′-TATGATCTCTCTGGTAACACAGC-3′	101 bp
		R 5′-TCAGGAACACAGACTCAGAC-3′	
Hdc	Histidine decarboxylase	F 5′-GTCAAGGACAAGTACAAGCTG-3′	84 bp
		R 5′-ATCTGCCAATGCATGAAGTC-3′	
Tac1	Tachykinin 1	F 5′-CAGCAGTTCTTTGGATTAATGG-3′	92 bp
		R 5′-CTGGCCATGTCCATAAAGAG-3′	
Th	Tyrosine hydroxylase	F 5′-AGCCCTACCAAGATCAAACC-3′	75 bp
		R 5′-GCATAGTTCCTGAGCTTGTC-3′	

Supplemental Table 2. *Expression levels of genes encoding the auxiliary subunits of the $Ca_v2.1$ channel in both tissues for both KI mice*

	Cerebellum		Occipital Cortex	
Gene	**R192Q[a]**	**S218L[a]**	**R192Q[a]**	**S218L[a]**
Genes encoding the auxiliary subunits				
Cacnb1	1.19 (0.06)	1.28 (0.007)*	-1.16 (0.03)*	-1.02 (0.68)
Cacnb2	1.1 (0.51)	-1.09 (0.29)	1.15 (0.11)	1.01 (0.85)
Cacnb3	1.05 (0.43)	1.04 (0.70)	-1.28 (0.03)*	-1.09 (0.42)
Cacnb4	1.05 (0.55)	-1.09 (0.39)	1.08 (0.64)	-1.19 (0.08)
Cacng1	1.07 (0.43)	-1.02 (0.78)	1.16 (0.08)	1.08 (0.32)
Cacng2	-1.06 (0.25)	-1.02 (0.67)	1.02 (0.50)	-1.04 (0.31)
Cacng3	1.04 (0.54)	-1.12 (0.35)	1.02 (0.88)	-1.14 (0.18)
Cacng4	1.06 (0.47)	1.09 (0.48)	-1.10 (0.38)	1.12 (0.35)
Cacng5	1.06 (0.39)	1.10 (0.13)	-1.16 (0.12)	1.12 (0.17)
Cacng6	-1.09 (0.78)	-1.31 (0.44)	-1.16 (0.54)	-1.46 (0.07)
Cacng7	1.12 (0.44)	-1.12 (0.46)	-1.26 (0.26)	-1.39 (0.04)*
Cacng8	-1.03 (0.85)	1.21 (0.10)	-1.12 (0.46)	-1.03 (0.75)
Cacna2d1	1.04 (0.76)	-1.29 (0.12)	1.24 (0.22)	-1.01 (0.74)
Cacna2d2	1.01 (0.83)	1.11 (0.13)	1.10 (0.27)	1.02 (0.80)
Cacna2d3	-1.01 (0.92)	1.06 (0.25)	-1.05 (0.29)	-1.04 (0.33)
Cacna2d4	1.09 (0.41)	1.01 (0.92)	-1.00 (0.99)	1.02 (0.68)

*[a]Fold change of respective mutant mice compared to wild-type mice, P-value for the respective fold change is indicated between brackets. *Fold-change with a $P < 0.05$*